THE JOURNAL OF BIOLOGICAL CHEMISTRY
Vol. 270, No. 51, Issue of December 22, pp. 30434–30440, 1995

Printed in U.S.A.

Kinetics of Oxidation of Tyrosine and Dityrosine by Myeloperoxidase Compounds I and II

IMPLICATIONS FOR LIPOPROTEIN PEROXIDATION STUDIES*

(Received for publication, July 13, 1995, and in revised form, September 11, 1995)

Leah A. Marquez and H. Brian Dunford‡

From the Department of Chemistry, University of Alberta, Edmonton, Alberta, Canada T6G 2G2

The oxidation of lipoproteins is considered to play a key role in atherogenesis, and tyrosyl radicals have been implicated in the oxidation reaction. Tyrosyl radicals are generated in a system containing myeloperoxidase, H_2O_2, and tyrosine, but details of this enzyme-catalyzed reaction have not been explored. We have performed transient spectral and kinetic measurements to study the oxidation of tyrosine by the myeloperoxidase intermediates, compounds I and II, using both sequential mixing and single-mixing stopped-flow techniques. The one-electron reduction of compound I to compound II by tyrosine has a second order rate constant of $(7.7 \pm 0.1) \times 10^5$ M^{-1} s^{-1}. Compound II is then reduced by tyrosine to native enzyme with a second order rate constant of $(1.57 \pm 0.06) \times 10^4$ M^{-1} s^{-1}. Our study further revealed that, compared with horseradish peroxidase, thyroid peroxidase, and lactoperoxidase, myeloperoxidase is the most efficient catalyst of tyrosine oxidation at physiological pH. The second order rate constant for the myeloperoxidase compound I reaction with tyrosine is comparable with that of its compound I reaction with chloride: $(4.7 \pm 0.1) \times 10^6$ M^{-1} s^{-1}. Thus, although chloride is considered the major myeloperoxidase substrate, tyrosine is able to compete effectively for compound I. Steady state inhibition studies demonstrate that chloride binds very weakly to the tyrosine binding site of the enzyme. Coupling of tyrosyl radicals yields dityrosine, a highly fluorescent stable compound that had been identified as a possible marker for lipoprotein oxidation. We present spectral and kinetic data showing that dityrosine is further oxidized by both myeloperoxidase compounds I and II. The second order rate constants we determined for dityrosine oxidation are $(1.12 \pm 0.01) \times 10^5$ M^{-1} s^{-1} for compound I and $(7.5 \pm 0.3) \times 10^2$ M^{-1} s^{-1} for compound II. Therefore, caution must be exercised when using dityrosine as a quantitative index of lipoprotein oxidation, particularly in the presence of myeloperoxidase and H_2O_2.

A major risk factor for coronary artery disease is an elevated level of low density lipoproteins (LDL),[1] the major carrier of blood cholesterol (1). Thus, the reduction of LDL levels has been a prominent preventive measure against atherosclerosis. However, evidence has accumulated indicating that oxidized LDL rather than native LDL triggers the pathological events leading to atherosclerosis (1–4). Foam cells or lipid-laden macrophages, derived from circulating monocytes, are the earliest cellular components of atherosclerotic lesions (5). It has been found that normal macrophages in culture cannot be converted to foam cells by simple incubation with even very high concentrations of native LDL. It is postulated that circulating LDL first undergo oxidative modification and then the oxidized LDL convert normal macrophages into foam cells (6, 7).

Myeloperoxidase, a heme protein abundant in phagocytes (8), is a potential physiological catalyst for lipoprotein oxidation (9, 10). Recent studies demonstrate links between myeloperoxidase and oxidative damage to proteins and lipids (11, 12). The identification of myeloperoxidase in human atherosclerotic lesions (13) is support for the hypothesis that myeloperoxidase is indeed involved in lipoprotein oxidation.

While myeloperoxidase follows the normal peroxidase cycle (14, 15),

$$MPO + H_2O_2 \rightarrow MPO\text{-}I + H_2O$$

$$MPO\text{-}I + AH_2 \rightarrow MPO\text{-}II + AH^{\cdot}$$

$$MPO\text{-}II + AH_2 \rightarrow MPO + AH^{\cdot} + H_2O$$

REACTION 1

where a single two-electron oxidation of native enzyme (MPO) to compound I (MPO-I) is followed by two successive one-electron reductions back to native enzyme via compound II (MPO-II), it shares an ability with eosinophil peroxidase (16) among the mammalian peroxidases in utilizing chloride to produce hypochlorous acid (17, 18),

$$MPO\text{-}I + Cl^- + H^+ \rightarrow MPO + HOCl + H_2O$$

REACTION 2

HOCl is a potent oxidizing agent that plays a cytotoxic role against invading bacteria, viruses, and tumor cells (8). However, it is also known to injure normal tissues by bleaching heme groups and oxidatively destroying electron transport chains (19) as well as chlorinating amino acids and unsaturated lipids (10, 20, 21). HOCl secreted by activated neutrophils can also cause oxidation of lipoproteins *in vivo* (22). Moreover, myeloperoxidase has been found to convert cholesterol to chlorohydrins and epoxides by a reaction involving HOCl (11).

Another potential lipoprotein oxidative pathway involving myeloperoxidase implicates the tyrosyl radical produced via one-electron oxidation of tyrosine by MPO-I (12, 23). When two tyrosyl radicals combine the major product is *o,o′*-dityrosine, an intensely fluorescent compound (24, 25). Fluorescence due to dityrosine has been observed in the reaction of tyrosine with

* This work was supported by the Natural Sciences and Engineering Research Council of Canada. The costs of publication of this article were defrayed in part by the payment of page charges. This article must therefore be hereby marked "*advertisement*" in accordance with 18 U.S.C. Section 1734 solely to indicate this fact.

‡ To whom correspondence should be addressed. Tel.: 403-492-3818; Fax: 403-492-8231; E-mail: Brian.Dunford@UAlberta.CA.

[1] The abbreviations used are: LDL/HDL, low/high density lipoprotein(s); MPO, MPO-I and MPO-II, myeloperoxidase and the oxidized enzyme intermediates compounds I and II; RZ, reinheitzahl (purity number).

linoleic acid 13-monohydroperoxide in the presence of methemoglobin (26). Dityrosine has also been detected in high density lipoproteins (HDL) treated with horseradish peroxidase, hydrogen peroxide, and tyrosine (27).

The concentration of free tyrosine in human blood plasma is 55 μM (28) and ranges from 22 to 83 μM in venous blood (29). Since dityrosine formation has been observed even in the presence of physiological concentrations of chloride (12, 30), the major MPO substrate, it has been suggested that tyrosine can be an effective reducing substrate for MPO. While the literature abounds with evidence for oxidative tyrosylation of lipoproteins (12, 23, 27, 30), limited if any details are reported on the myeloperoxidase-catalyzed one-electron oxidation of tyrosine. In this paper we report spectral and transient kinetic data for the oxidation of tyrosine by the MPO/H_2O_2 system. Rate constant determination for MPO-I reactions were made possible by employing sequential mixing stopped-flow techniques. We also report rate constants for tyrosine oxidation by MPO-II. The contribution of this reaction to tyrosyl-mediated lipid peroxidation has never received attention to the best of our knowledge. Moreover, the retention of the phenolic groups in the tyrosine oxidation product, dityrosine, raises the possibility of further oxidation. Herein we also report rate constants for dityrosine oxidation by both MPO-I and MPO-II. These data will be useful in evaluating the stability of the end product dityrosine, which has been proposed as a possible marker for lipid peroxidation (30) or as an index of oxidative damage to proteins *in vivo* and *in vitro* (31, 32). Since chloride is considered the major substrate of myeloperoxidase *in vivo*, we also investigated the steady state rates of tyrosine oxidation in the presence and absence of chloride. By use of a sequential-mixing stopped-flow instrument we have measured the rate constant for MPO-I reaction with chloride previously unreported in the literature. These results not only contribute quantitative support to the accumulating evidence on the role of tyrosyl radicals in lipoprotein peroxidation but also present differences in tyrosine oxidation by MPO compared with other peroxidases.

EXPERIMENTAL PROCEDURES

Materials—Bovine spleen myeloperoxidase was isolated and purified using a combination of modified procedures (33–36). The enzyme preparation used in this study exhibited an RZ (A_{429}/A_{280}) of 0.83. The MPO concentration was determined spectrophotometrically using an extinction coefficient of 178 mM^{-1} cm^{-1} at 429 nm (37).

Diluted hydrogen peroxide, obtained as a 30% solution from BDH Chemicals, was standardized using the horseradish peroxidase-catalyzed oxidation of iodide to triiodide (38). Concentrations were confirmed using absorbance measurements at 240 nm where the extinction coefficient of H_2O_2 is 39.4 M^{-1} cm^{-1} (39). Ultrapure L-tyrosine was obtained from Sigma. KCl (Aldrich) and the chemicals used for the buffers (Fisher) were used without further purification. Aqueous solutions were prepared using water purified through the Milli-Q system (Millipore Corp.), and concentrations of solutes were determined by weight.

Dityrosine was prepared using a combination of published procedures (24, 40, 41). 1.0 gram of L-tyrosine was dissolved in 910 ml of water, and then 50 ml of 0.1% H_2O_2 and 40 mg of horseradish peroxidase (Type VI-A, Sigma) were added. The pH was adjusted to 9.2 using 6 M NaOH, and the mixture was incubated in a thermostated bath for 17 h at 37 °C. At the end of the reaction the pH was adjusted to 6.0 with concentrated HCl. The mixture was concentrated almost to dryness in a rotatory evaporator under vacuum at 40 °C. Water was added to the concentrate to a volume of 60 ml. The mixture was treated with 2 g of Darco G-60 activated charcoal (Aldrich) and left standing overnight. Centrifugation at 10,000 rpm for 15 min using the JA-20 rotor of Beckman model J2-21 preparative centrifuge yielded a clear yellowish brown supernatant. This was then applied to a precycled P-11 cellulose phosphate cationic exchanger (Whatman) column (1.5 × 35 cm), which had been previously equilibrated with 0.2 M acetic acid. Elution of the column was performed with 0.2 M acetic acid containing 0.5 M NaCl at a flow rate of 15 ml/h. Fractions of 3 ml were collected and evaluated spectrophotometrically at 280 and 310 nm. Samples of the major peak fractions were transferred on thin layer silica gel plates (Whatman). After developing the plates in *n*-butyl alcohol/acetic acid/water (4:1:1, v/v) the fractions were pooled that were positive for ninhydrin and with R_f value (the ratio of the distance traveled by the band to the distance traveled by the mobile phase) of about 0.15. The solution was applied to a Dowex 50 × 8 (Terochem) column previously soaked in 0.1 M HCl. The column was extensively washed with water to remove all NaCl and acetic acid. The dityrosine was subsequently eluted with 2 M ammonia. Eluates were evaluated spectrophotometrically as before. Samples of major peak fractions were applied on thin layer silica gel plates, and the fractions with R_f values of about 0.12 were pooled. The solvent was removed in a rotatory evaporator under vacuum. The concentrate of dityrosine was characterized by thin layer chromatography, ultraviolet spectroscopy and fluorescence measurements (42). Final concentrations were determined by measuring absorbance at 315 nm using an extinction coefficient of 5.2 mM^{-1} cm^{-1} at pH 7.5 (43).

Methods—Routine absorbance measurements were made on a Beckman DU-650 spectrophotometer equipped with thermally jacketed 1-cm cuvette holders. Rapid spectral scans and kinetic measurements were performed using the SX.17 MV microvolume stopped-flow spectrofluorimeter (Applied Photophysics). Time-dependent spectra from single wavelength shots were reconstructed using the GLint application software. A 1-cm path length was used for absorbance measurements, and a 2-mm path length was used for fluorescence measurements. All experiments were carried out at 20.5 ± 0.5 °C, ionic strength of 0.1 M, and pH 7.4 (phosphate buffer) unless otherwise specified. All pH measurements were made using a Fisher Accumet model 25 digital pH meter.

The kinetics of the reactions of MPO-I with tyrosine and dityrosine were carried out using the sequential mixing mode of the stopped-flow apparatus. 1.0 μM of myeloperoxidase was premixed with 20 μM H_2O_2 in 0.1 M phosphate buffer. After a delay time of 20 ms the formed MPO-I was allowed to react with varying concentrations of L-tyrosine or dityrosine, the final concentrations of which were at least 10-fold in excess of the enzyme intermediate. The time course of the reaction was followed by monitoring the absorbance changes at 456 nm accompanying the formation of MPO-II. This wavelength is also the isosbestic point between native enzyme and MPO-I (36).

The reaction of MPO-I with chloride was investigated at 429 nm, the isosbestic point between MPO-I and MPO-II, which also corresponds to the maximum change in absorbance as MPO-I undergoes a two-electron reduction back to the native enzyme. Pseudo-first order rate constants, k_{obs}, were determined using the single exponential curve-fit equation of the Applied Photophysics software. Five or six determinations of rate constants were performed for each reducing substrate concentration, and the mean values were plotted against the substrate concentration. The apparent second order rate constants for the MPO-I reactions were calculated from the slopes using linear least squares regression analysis (Enzfitter, Elsevier-Biosoft).

MPO-II reactions with L-tyrosine and dityrosine were carried out using the single-mixing mode of the stopped-flow apparatus. Prior to the kinetic experiments the stability of preformed MPO-II was studied by wavelength scanning using the Beckman spectrophotometer. MPO-II was prepared by adding a 50-fold excess of H_2O_2 to native enzyme and then allowing this enzyme intermediate to react with tyrosine and dityrosine under pseudo-first order conditions. Kinetic measurements were made at 456 nm where the maximum change in absorbance is observed as MPO-II is converted back to native enzyme. Pseudo-first order rate constants were determined from seven or more exponential traces, and second order rate constants were calculated as before.

Steady state experiments on the oxidation of tyrosine by the MPO/H_2O_2 system were conducted by following the initial rate of formation of dityrosine. The reaction was monitored by measuring the increase in fluorescence with time using wavelengths of 325 and 405 nm for excitation and emission. In a typical experiment one syringe contained MPO and tyrosine in phosphate buffer while the other contained H_2O_2. To determine the effect of chloride, known concentrations of KCl solution were added to the syringe containing H_2O_2. The final concentrations after mixing were 25 nM MPO, 50 μM H_2O_2, 0.2–1.0 mM tyrosine, and 0–0.125 M KCl. The initial rates were determined from the slopes of the first linear portions of the traces obtained after mixing all the components. The dead time of the instrument was ~1.5 ms. Usually six to eight traces were recorded, and the mean values of the initial rate of increase in fluorescence with time were calculated. A calibration curve of fluorescence signal (volts) against dityrosine concentration is linear up to 20 μM dityrosine. By interpolation, initial rates in fluorescence units were converted to rates in terms of dityrosine concentration. Double reciprocal plots as well as Dixon plots were constructed to

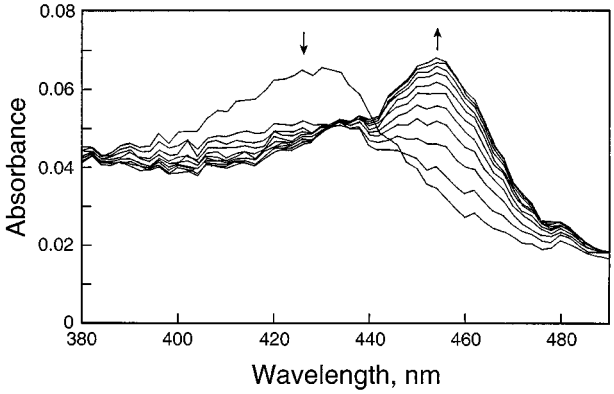

FIG. 1. **Rapid scan spectra of MPO-I reduction to MPO-II by tyrosine.** One syringe contained 1.0 μM MPO and 50 μM tyrosine in phosphate buffer while the other had 20 μM H_2O_2 in the same buffer. The *arrows* show the direction of absorbance changes with time. The first, second, and last scans were taken 2.5, 10, and 100 ms after mixing.

determine the type of inhibition chloride exerts on tyrosine oxidation (44).

RESULTS

Preliminary wavelength scans of myeloperoxidase in phosphate buffer in the absence and presence of tyrosine or dityrosine revealed no interference in the wavelengths to be used for transient kinetic measurements (spectra not shown). Kinetic scans of the reaction between native MPO and H_2O_2 in the presence of tyrosine are shown in Fig. 1. The first scan is that of native enzyme, and the second scan is that of MPO-I. The succeeding scans demonstrate the rapid reduction of MPO-I to MPO-II. MPO-I formation takes place within 10 ms after mixing, followed by its conversion to MPO-II, which is completed in 100 ms. Full formation of MPO-I is achieved only in the presence of a 20-fold excess of H_2O_2 (36). However, since MPO-I is also spontaneously reduced to MPO-II in the presence of excess H_2O_2 it was necessary to determine the rate of reduction of MPO-I by tyrosine relative to its rate of spontaneous decay. The instability of MPO-I necessitated the use of the sequential mixing stopped-flow apparatus. The premixing of MPO and H_2O_2 led to MPO-I formation within 20 ms, and before the MPO-I decayed it allowed the measurement of the rate of the subsequent reaction of MPO-I with a reducing substrate.

The time courses for the reduction of MPO-I to MPO-II may be followed by monitoring the disappearance of MPO-I at 442 nm, the isosbestic point between MPO and MPO-II, or the formation of MPO-II at 456 nm, the isosbestic point between MPO and MPO-I. Rate constants obtained in both cases are the same within experimental uncertainty (36). We chose to perform kinetic measurements for MPO-I reduction by tyrosine at 456 nm because the absorbance change accompanying MPO-II formation at this wavelength is larger and leads to smaller experimental errors. A typical kinetic trace displaying single exponential character is shown in the *inset* to Fig. 2. The apparent second order rate constant was obtained from the slope of the plot of pseudo-first order rate constants, k_{obs}, against tyrosine concentration (Fig. 2): $(7.7 \pm 0.1) \times 10^5$ M^{-1} s^{-1}. A value of $(6.3 \pm 0.2) \times 10^5$ M^{-1} s^{-1} was obtained using the single-mixing mode of the apparatus. However, the intercept of the plot obtained using the single-mixing mode is bigger, 9.5 ± 1.8 s^{-1}, compared with 2.2 ± 1.2 s^{-1} (Fig. 2), obtained using the sequential-mixing mode. The value of the intercept indicates the rate of the spontaneous reduction of MPO-I by excess H_2O_2 in the absence of tyrosine. Thus, the use of sequential mixing stopped-flow minimized the interference of MPO-I reduction to

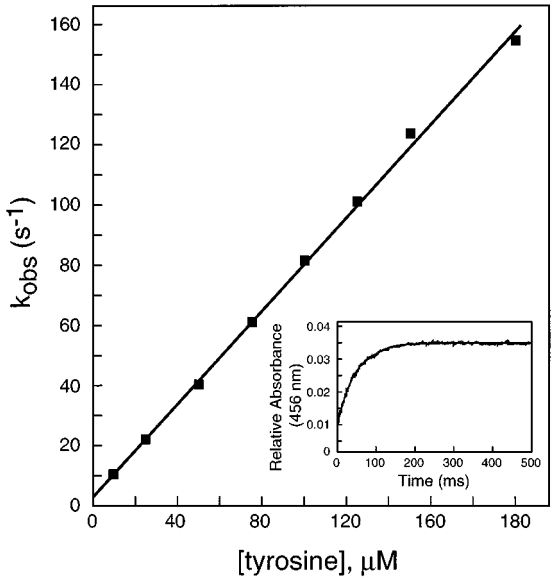

FIG. 2. **Pseudo-first order rate constants for MPO-I reduction by tyrosine.** The *inset* shows a typical trace and curve fit (*solid line*) of the reaction followed at 456 nm using sequential mixing mode. Final concentrations were 0.25 μM MPO, 5 μM H_2O_2 (μ = 0.1 M due to phosphate buffer, pH 7.4). The second order rate constant was calculated from the slope. The standard deviations of the k_{obs} values ranged from 0.5 to 3.5%.

MPO-II by excess H_2O_2.

The rate constant for MPO-I reduction by tyrosine at pH 7.4 was higher than the rate at pH 4.5, the pH inside the phagocyte (45). We performed pseudo-first order rate measurements at single tyrosine concentrations from pH 3.0 to 8.8, and the results are presented in Fig. 3.

While MPO-I is thermodynamically competent to form tyrosyl radicals via its one-electron oxidation of tyrosine (17), the capability of MPO-II to generate tyrosyl radicals was unknown (12). MPO-II is more stable than MPO-I (36, 46, 47). A good preparation of MPO-II is obtained by adding a 50-fold excess of H_2O_2 to pure native enzyme. The MPO-II spectra remained basically unchanged after 10 min (Fig. 4). Upon addition of tyrosine, MPO-II is rapidly reduced to native enzyme. This one-electron enzyme reduction must be accompanied by a one-electron oxidation of the reducing substrate. These results prove that MPO-II is also capable of oxidizing tyrosine and generating tyrosyl radicals.

Because of the relative stability of MPO-II we were able to conduct rate measurements of the reaction of MPO-II with tyrosine using the single-mixing mode of the stopped-flow apparatus. The monophasic exponential decrease in absorbance at 456 nm with time as MPO-II is converted back to native enzyme yielded k_{obs} values that were plotted against tyrosine concentration as before (data not shown). The plot was linear up to 250 μM tyrosine, and the intercept is zero within the standard deviations of the measurements. The second order rate constant for the reaction of MPO-II with tyrosine obtained from the slope of the plot was $(1.57 \pm 0.06) \times 10^4$ M^{-1} s^{-1}.

Dityrosine has been detected in the MPO/H_2O_2 system of human neutrophils and macrophages as a product of tyrosyl radical coupling (30). Aside from the dimer, other polymeric products have been identified in sytems employing horseradish peroxidase (25) and ovoperoxidase (48). It was of interest to determine whether MPO would further catalyze the oxidation of dityrosine since the phenolic groups are retained in the dimer.

Dityrosine was prepared enzymatically, purified, and characterized (42). For the kinetic measurements it is important to

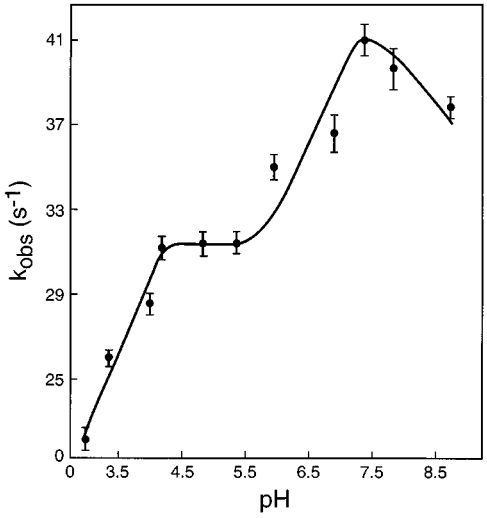

FIG. 3. **pH dependence of pseudo-first order rate constants for MPO-I reduction by tyrosine.** Final concentrations were 0.5 μM MPO, 10 μM H_2O_2, 50 μM tyrosine in 0.1 M buffer. The buffers used were citrate (pH 3.0–5.4), phosphate (pH 6.0–7.8), and carbonate (pH 8.8).

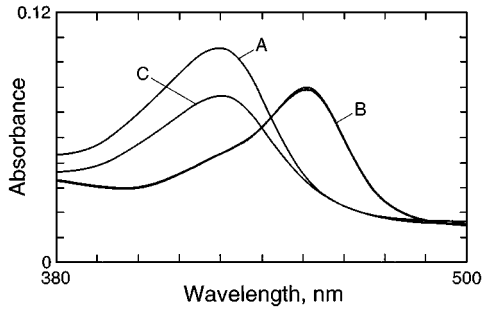

FIG. 4. **Wavelength scan of the reaction between MPO-II and tyrosine.** *Scan A* is for MPO (0.5 μM in 0.1 M phosphate buffer). Consecutive *scans B* (MPO-II) were taken within a time period of 10 min after adding 25 μM H_2O_2 to MPO. *Scan C* was taken immediately after the addition of 50 μM tyrosine to MPO-II.

work with authentic dityrosine freed of tyrosine impurities. Dityrosine is easily monitored by its characteristic fluorescence at 400 nm (49). It also shows maximum absorbance at 285 nm in acid solution and at 315 in alkaline solution (26). Dityrosine yields a single ninhydrin-positive spot on silica gel with R_f of 0.12 when using *n*-butyl alcohol/acetic acid/water (4:1:1 v/v) as a solvent system (42, 50). All of these criteria were satisfied by the dityrosine used in this work.

The addition of dityrosine to preformed MPO-II resulted in conversion of MPO-II to native enzyme, although not as fast compared with the reaction of tyrosine. A shoulder at 456 nm in the wavelength scans (Fig. 5, *inset*) indicates that MPO-II reduction is not complete within the time period of the scan. Similar rate measurements under pseudo-first order conditions were conducted for the reactions of MPO-I and MPO-II with dityrosine. The second order rate constant determined from the slope of the plot of k_{obs} against dityrosine concentration for the MPO-II reaction is $(7.5 \pm 0.3) \times 10^2$ M^{-1} s^{-1} (Fig. 5). The second order rate constant for the MPO-I reaction with dityrosine was more than 2 orders of magnitude larger: $(1.12 \pm 0.01) \times 10^5$ M^{-1} s^{-1}.

The major reducing substrate for MPO is considered to be chloride, the oxidation product of which is hypochlorous acid (8). It has been suggested that chloride inhibits the initial rate of oxidation of tyrosine by myeloperoxidase (30). It is relevant to evaluate the relative rates of tyrosine and chloride oxidation by MPO-I. By using sequential mixing stopped-flow measure-

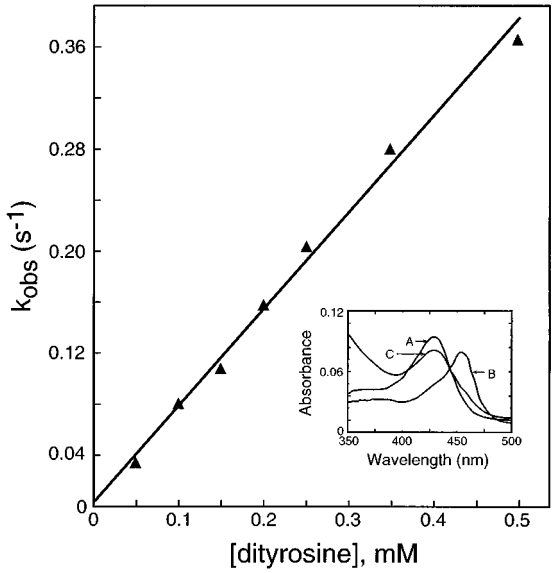

FIG. 5. **Determination of rate constant for the reaction of MPO-II with dityrosine.** Pseudo-first order rate constants were determined upon mixing MPO-II (prepared by adding 25 μM H_2O_2 to 0.5 μM MPO) with varying concentrations of dityrosine. The *inset* shows wavelength scans for the reaction. *Scan A* is for 0.5 μM MPO in 0.1 M phosphate buffer; *scan B* (MPO-II) was taken after 10 μM H_2O_2 was added to the native enzyme; and *scan C* was taken after adding 50 μM dityrosine to MPO-II.

ments we determined the second order rate constant for MPO-I oxidation of chloride to be $(4.7 \pm 0.1) \times 10^6$ M^{-1} s^{-1}. Unlike previous plots, which had nearly zero intercepts (Figs. 2 and 5, for example), the plot of k_{obs} *versus* chloride concentration yielded an intercept of (31 ± 4) s^{-1} (data not shown).

We were also interested in the type of inhibition chloride exerts on tyrosine oxidation. This was investigated under steady state conditions by monitoring the rate of formation of the dityrosine oxidation product in a system containing MPO, H_2O_2, tyrosine, and chloride. The rate of dityrosine formation may be followed by monitoring absorbance changes at 315 nm (43) or fluorescence changes using 325 and 405 nm as excitation and emission wavelengths. The fluorescence signal is larger, so we chose it over absorbance to measure initial rates of dityrosine formation. Fig. 6 shows that tyrosine does not contribute to the fluorescence reading. The concentration of dityrosine in the reaction mixture was interpolated from a calibration curve of purified dityrosine (Fig. 6, *inset*).

The initial rate of tyrosine oxidation was measured as a function of tyrosine concentration, and the results are shown in Fig. 7. Obviously, the plot is not hyperbolic and therefore does not yield corresponding Michaelis-Menten parameters. Double reciprocal plots of initial rates against tyrosine concentration increase in slope as the concentration of chloride increases (Fig. 8). A secondary plot of the slopes from the double reciprocal plots against chloride concentration (Fig. 8, *inset*) yields an inhibitor constant K_i equal to 0.16 M. Values of K_i are usually obtained accurately by using Dixon plots (51), *i.e.* plots of the reciprocal of initial rate against inhibitor concentration at various fixed concentrations of substrate. The family of Dixon plots in Fig. 9 suggests either competitive or linear mixed-type inhibition (44), and from the point of intersection we obtained the inhibition constant of chloride, $K_i = 0.18 \pm 0.02$ M; and the maximum velocity for tyrosine oxidation, $V_{max} = 1.7 \pm 0.1$ μM dityrosine $\cdot$ s^{-1}.

DISCUSSION

The peroxidase-catalyzed oxidation of tyrosine has recently attracted renewed interest due to its involvement in lipid and

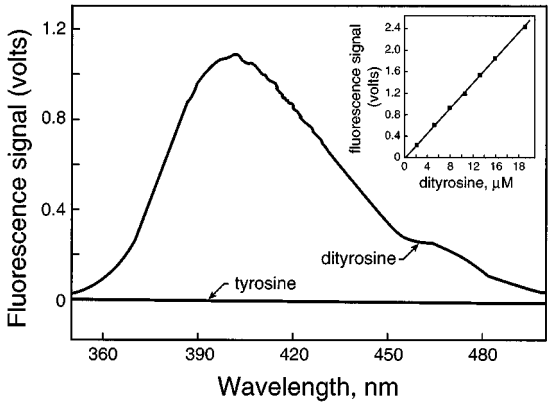

FIG. 6. **Fluorescence spectra of dityrosine.** The excitation wavelength was set at 325 nm. Tyrosine does not fluoresce when exposed to 325-nm light. The *inset* shows the calibration curve used for calculating dityrosine concentration from fluorescence readings.

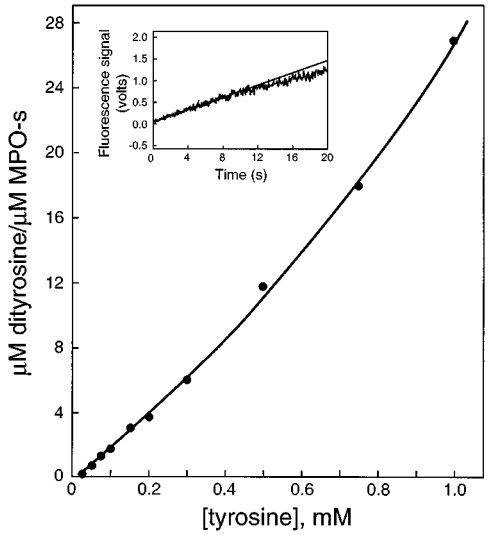

FIG. 7. **Steady state initial rates of dityrosine formation.** Final concentrations were 25 nM MPO, 0.1 mM H_2O_2 at 0.1 M phosphate. The initial rates were determined from the slope of the initial portion of the trace of increase in fluorescence with time (*inset*, 1 mM tyrosine was used).

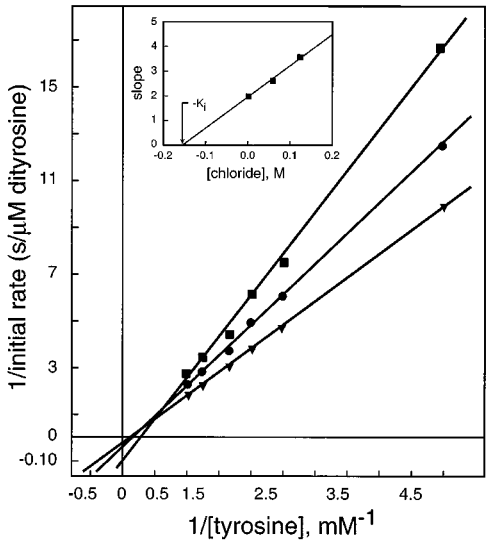

FIG. 8. **Double reciprocal plots for chloride inhibition of dityrosine formation.** Final concentrations were 25 nM MPO, 50 μM H_2O_2 at 0.1 M phosphate; chloride concentrations (in M) were 0 (▼), 0.06 (●), and 0.125 (■). *Inset* is a replot of the slopes from the reciprocal plots against chloride concentration. The *x* intercept gives the negative value of K_i.

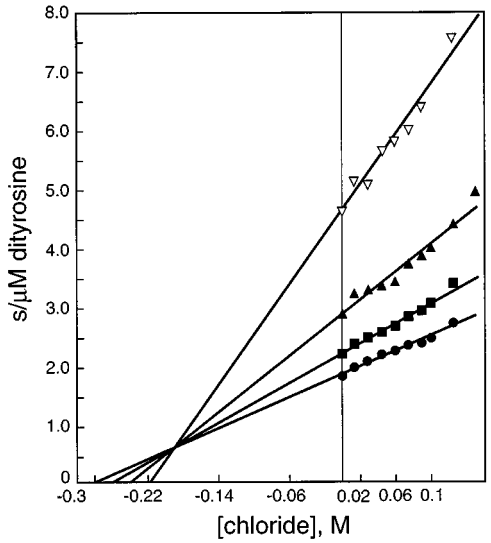

FIG. 9. **Dixon plots for chloride inhibition.** Final concentrations are as in Fig. 8. Tyrosine concentrations (in mM) were 0.4 (▽), 0.6 (▲), 0.8 (■), and 1.0 (●).

protein oxidation (12, 27, 31). The oxidation of tyrosine has also been implicated in the biosynthesis of thyroxine and melanin (43) and in the cross-linking of structural proteins via the dityrosine linkage (for a review see Ref. 42). Previous investigations of the kinetics of tyrosine oxidation have been performed using lactoperoxidase (43, 52), horseradish peroxidase (53, 54), and thyroid peroxidase (52, 55). Our present work provides the first report of the rate constants for the oxidation of tyrosine as catalyzed by myeloperoxidase. These results are significant in lieu of the findings that MPO has been identified as a physiological catalyst for lipid peroxidation in low density lipoproteins via tyrosyl radicals (12, 23).

While all hemoprotein peroxidases are generally considered to catalyze oxidation reactions in a similar manner, Table I shows varying values in the rate constants for the oxidation of tyrosine by several peroxidases under similar pH and temperature conditions. This reflects differences in the effectiveness of various peroxidases in catalyzing the oxidation of tyrosine. Horseradish peroxidase is the least effective catalyst for tyrosine oxidation. Among the three mammalian peroxidases, thyroid peroxidase has the lowest rate constant for compound I reduction by tyrosine. This is to be expected because the primary reaction catalyzed by thyroid peroxidase is iodination of the tyrosyl residues in thyroglobulin; therefore, tyrosine oxidation may not be as important. Moreover, thyroid peroxidase has a unique property of catalyzing the two-electron oxidation of tyrosine (55), which differentiates it from lactoperoxidase and myeloperoxidase, which oxidize tyrosine via two successive one-electron processes. The rapid spectral scans of the MPO/H_2O_2 system in the presence of tyrosine (Fig. 1) clearly show

TABLE I
Second order rate constants ($M^{-1}s^{-1}$) for the reduction of compounds I and II of various peroxidases by tyrosine, with references

All experiments were performed in phosphate buffer. pH and temperature conditions are as follows: pH 8.2 and 25 °C (43); pH 7.5 and 20 °C (52); pH 7.5 and 25 °C (53, 54); pH 7.4 and 20 °C (this work).

	Compound I	Compound II
Horseradish peroxidase	5.0×10^4 (53)	1.1×10^3 (54)
Lactoperoxidase	$>1.1 \times 10^5$ (52)	1.03×10^4 (43)
Thyroid peroxidase	7.5×10^4 (52)	4.3×10^2 (52)
Myeloperoxidase	7.72×10^5 (this work)	1.57×10^4 (this work)

that MPO-I undergoes a one-electron reduction to MPO-II followed by the slower one-electron reduction of MPO-II to native enzyme (Fig. 4).

The rate constant for lactoperoxidase compound-I reaction with tyrosine could only be estimated by previous workers (52) due to the inherent instability of its compound I. We were able to overcome this problem in our transient kinetic measurements through the use of a sequential mixing stopped-flow apparatus. Our data establish that myeloperoxidase is the most effective among the mammalian peroxidases in catalyzing both the one-electron reductions of its compounds I and II by tyrosine. Our results also show that tyrosine could contribute to the turnover of MPO-II to native enzyme in the absence of other reducing substrates.

Another striking difference displayed by these peroxidases in their oxidation of tyrosine is the pH at which the maximum rate is observed for compound I reduction. For horseradish peroxidase, the maximum rate is at pH 9.6 (53), while for lactoperoxidase it is at pH 8.2 (43). Fig. 3 indicates that for MPO, the maximum rate is achieved at the physiological pH of 7.4. In a related study of the pH dependence, the formation of dityrosine, the stable primary product of the myeloperoxidase-catalyzed oxidation of tyrosine, was found to be highest at pH 7.5–8.0 (30). Apparently, oxidation of tyrosine requires deprotonation of its phenolic hydroxyl group (56). Thus, inside the acidic environment of the phagosome (45) the predominant reaction is not likely tyrosine oxidation but rather chloride oxidation by MPO-I to form HOCl. Moreover, it has been demonstrated that only at acidic pH is there direct contact between chloride and ferryl oxygen in MPO-I resulting in a maximum rate of HOCl formation (57).

MPO-I and MPO-II are each able to oxidize tyrosine in a one-electron reaction to give tyrosyl radicals. Long-lived tyrosyl radicals have also been produced by chemical oxidation of tyrosine using ferricyanide and characterized by electron spin resonance (58). However, the readily detectable product of tyrosine oxidation is *o,o′*-dityrosine formed by coupling of phenoxy radicals (25). Dityrosine is intensely fluorescent (Fig. 6), and in proteins it has been found to be resistant to proteolysis (31), to borohydride treatment (26), and to acid hydrolysis (30). Because of its apparent stability dityrosine has been proposed as a chemical marker of cumulative exposure of proteins to metal-catalyzed oxidation *in vitro* and *in vivo* (32), an index of organismal oxidative stress (31), and an indication of targets where phagocytes inflict oxidative damage *in vivo* (30). However, it is also known that extensive action of peroxidases on tyrosine results in the formation of other oxidation products such as trityrosine and other polymers, some of which are also fluorescent (25, 30, 43, 48). This is probably the reason why the steady state rates of dityrosine formation measured by the increase in fluorescence did not reach saturation but continued to increase with time (Fig. 7).

Since the phenoxy groups are retained in dityrosine it is likely that dityrosine can be further oxidized by the MPO/H_2O_2 system. The *inset* to Fig. 5 shows that dityrosine can reduce MPO-II to native enzyme, although the rate would not seem physiologically relevant. On the other hand the rate constant for MPO-I reaction with dityrosine yields a value, $(1.12 \pm 0.01) \times 10^5$ M^{-1} s^{-1}, which is not significantly lower than the reaction of MPO-I with tyrosine. The lower rate constant for the more bulky dityrosine substrate is consistent with the finding that aromatic substrate molecules bind at the distal heme pocket of myeloperoxidase (59) and that this site exhibits considerable steric hindrance (17). The fast oxidation of dityrosine by MPO-I suggests that dityrosine may not be a very stable end product and that it should be used with caution as a marker for oxidative damage, particularly in the presence of the MPO/H_2O_2 system.

Since the major physiological substrate of MPO is considered to be chloride, we also evaluated the relative rates of tyrosine and chloride oxidation by MPO-I. There have been difficulties in obtaining the rate constant for the two-electron oxidation of chloride by MPO-I. Full formation of MPO-I is achieved only in the presence of at least a 20-fold excess of H_2O_2 over MPO (30). But with excess H_2O_2, MPO-I is reduced at a very fast rate to MPO-II, making it difficult to measure the rate constant for the MPO-I reaction with chloride. We were able to overcome this problem by using the sequential mixing mode of the stopped-flow apparatus. The second order rate constant for chloride peroxidation by MPO-I, $(4.7 \pm 0.1) \times 10^6$ M^{-1} s^{-1}, is about an order of magnitude higher than the rate constant for tyrosine oxidation by MPO-I and about the same value as the rate constant for the formation of an MPO-chlorinating intermediate $(2.8 \pm 1.2) \times 10^6$ M^{-1} s^{-1} (60). However, unlike the other plots of k_{obs} against substrate concentration, which had zero intercepts within experimental error (Figs. 2 and 5, for example), the plot for the chloride reaction with MPO-I yielded a considerable *y* intercept (31 ± 4) s^{-1}. This suggests a reversible reaction. In fact, the oxidation product of chloride, HOCl, can undergo a rapid reaction with native MPO to give MPO-I, which is ostensibly the reverse of the chloride peroxidation reaction (17, 18).

For the chloride inhibition studies we constructed both double reciprocal and Dixon plots, which are used to identify the type of inhibition and to determine the inhibition constant, K_i (51). The two types of plots only establish that the inhibition is neither noncompetitive nor uncompetitive. The data are characteristic of either purely competitive or mixed-type inhibition (44). The replot of the slopes of the Dixon plots against reciprocal of substrate (tyrosine) concentration did not umambiguously predict which type of inhibition is occurring. The Cornish-Bowden plot (61) (graphs not shown) did not clarify the kind of inhibition either. Indeed it may be difficult to characterize the type of inhibition in such a complex system where the enzyme is in contact with three substrates: H_2O_2, tyrosine, and chloride. A simple interpretation of plots used for inhibition studies is not possible for multisubstrate systems (61), and especially where the products (HOCl and dityrosine) are also substrates. H_2O_2 and chloride have been shown to be competitive inhibitors of each other (62–64). The substrate inhibition patterns of these studies suggest the existence of two binding sites for chloride; one is a substrate binding site and the other an inhibitor binding site. The binding of chloride to its substrate binding site results in the production of HOCl, whereas its binding to the inhibitor binding site leads to competitive inhibition of H_2O_2 binding to native MPO. Inhibition by chloride almost certainly involves coordination to the heme because MPO-I has a ferryl oxygen occupying the sixth coordination position and possesses no available chloride binding sites. The catalytic site for chloride peroxidation is most likely located within the distal heme cavity (57) or at the heme periphery (17, 65). Recently, EPR spectroscopy and model building revealed that the hydrophobic character of the entrance to the distal cavity of MPO allows favorable interaction with aromatic molecules (59) such as tyrosine. If indeed the chloride substrate binding site is in the distal heme pocket, then it would compete with tyrosine. However, the large value of K_i we obtained in our steady state studies suggests that binding of chloride is very weak, presumably because of the hydrophobic nature of the pocket. That would explain why tyrosine oxidation takes place at considerable rates even in the presence of high concentrations of chloride. These results are consistent with the findings

that tyrosine oxidation occurs even in the presence of physiological concentrations of chloride (12, 30) and that LDL oxidation by tyrosyl radicals is largely unaffected by as high as 0.1 M chloride present in the plasma (23).

In conclusion, both MPO-I and MPO-II are able to react with tyrosine via one-electron oxidations and therefore generate tyrosyl radicals. The relatively fast rate of the MPO-I reaction with tyrosine substantiates the conjecture that tyrosine oxidation by MPO-I takes place *in vivo* and may be physiologically relevant. Tyrosine also competes very effectively with the major myeloperoxidase substrate chloride. That tyrosine can also reduce MPO-II to native enzyme ensures turnover of the enzyme even in the absence of other reducing substrates. The tyrosyl radical formed in both reactions is a diffusible catalyst that can convey oxidizing potential away from the active site of the heme enzyme. A protein tyrosyl radical has been implicated in cross-linking of proteins (12), in initiating lipid peroxidation in LDL (23) and modifying HDL to protect the arterial wall against cholesterol accumulation (27). The readily detectable product of tyrosine oxidation is dityrosine formed by the coupling of tyrosyl radicals. Our study revealed that since dityrosine is further oxidized at a very fast rate by MPO-I caution must be exercised when using it as a quantitative index of lipoprotein modification. It would appear to measure a lower limit of lipoprotein modification.

REFERENCES

1. Heinecke, J. W. (1987) *Free Radical Biol. & Med.* **3,** 65–73
2. Zhang, H., Yang, Y., and Steinbrecher, U. P. (1993) *J. Biol. Chem.* **268,** 5535–5542
3. Steinberg, D., Parthasarathy, S., Carew, T. E., Khoo, J. C., and Witztum, J. E. (1989) *N. Eng. J. Med.* **320,** 915–924
4. Ylä-Herttuala, S., Palinski, W., Rosenfeld, M. E., Parthasarathy, S., Carew, T. E., Butler, S., Witztum, J. L., and Steinberg, D. (1989) *J. Clin. Invest.* **84,** 1086–1095
5. Ross, R. (1986) *N. Eng. J. Med.* **314,** 488–500
6. Hazell, L. J., and Stocker, R. (1993) *Biochem. J.* **290,** 165–172
7. Steinbrecher, U. P., Parthasarathy, S., Leake, D. S., Witztum, J. L., and Steinberg, D. (1984) *Proc. Natl. Acad. Sci. U. S. A.* **81,** 3883–3887
8. Klebanoff, S. J., and Clark, R. A. (1978) *The Neutrophil: Function and Clinical Disorders*, North-Holland Publishing Co., Amsterdam
9. Stelmaszynska, T., Kukovetz, E., Egger, G., and Schaur, R. J. (1992) *Int. J. Biochem.* **24,** 121–128
10. Winterbourn, C. C., Vandenberg, J. J. M., Roitman, E., and Kuypers, F. A. (1992) *Arch. Biochem. Biophys.* **296,** 547–555
11. Heinecke, J. W., Li, W., Mueller, D. M., Bohrer, A., and Turk, J. (1994) *Biochemistry* **33,** 10127–10136
12. Heinecke, J. W., Li, W., Francis, G. A., and Goldstein, J. A. (1993) *J. Clin. Invest.* **91,** 2866–2872
13. Daugherty, A., Dunn, J. L., Rateri, D. L., and Heinecke, J. W. (1994) *J. Clin. Invest.* **94,** 437–444
14. Poulos, T. L., and Fenna, R. E. (1994) in *Metals in Biological Systems*, Vol. 30 (Siegel, H., ed) pp. 25–75, Marcel Dekker, New York
15. Dunford, H. B. (1991) in *Peroxidases in Chemistry and Biology*, Vol. II (Everse, J., and Grisham, M. B., eds) pp. 1–24, CRC Press, Boca Raton, FL
16. Wever, R., Plat, H, and Hamers, M. N. (1981) *FEBS Lett.* **123,** 327–331
17. Hurst, J. K., and Barrette, W. C., Jr. (1989) *Crit. Rev. Biochem. Mol. Biol.* **24,** 271–328
18. Harrison, J. E., and Schultz, J. (1976) *J. Biol. Chem.* **251,** 1371–1374
19. Albrich, J. M., McCarthy, C. A., and Hurst, J. K. (1981) *Proc. Natl. Acad. Sci. U. S. A.* **78,** 210–214
20. Thomas, E. L., Jefferson, M. M., and Grisham, M. B. (1982) *Biochemistry* **21,** 6299–6308
21. Zgliczynski, J. M., Stelmaszynska, T., Domanski, J., and Ostrowski, W. (1971) *Biochim. Biophys. Acta* **235,** 419–424
22. Panasenko, O. M., Evgina, S. A., Aidyraliev, R. K., Sergienko, V. I., and Vladimirov, Y. A. (1994) *Free Radical Biol. & Med.* **16,** 143–148
23. Savenkova, M. I., Mueller, D. M., and Heinecke, J. W. (1994) *J. Biol. Chem.* **269,** 20394–20400
24. Andersen, S. O. (1966) *Acta Physiol. Scand.* **66**, Suppl. 263, 1–81
25. Gross, A. J., and Sizer, I. W. (1959) *J. Biol. Chem.* **234,** 1611–1614
26. Kikugawa, K., Kato, T., and Hayasaka, A. (1991) *Lipids* **26,** 922–929
27. Francis, G. A., Mendez, A. J., Bierman, E. L., and Heinecke, J. W. (1993) *Proc. Natl. Acad. Sci. U. S. A.* **90,** 6631–6635
28. Soupart, P. (1962) in *Amino Acid Pools: Distribution, Formation and Function of Free Amino Acids* (Holden, J. T., ed) pp. 220–262, Elsevier Publishing Co. Inc., Amsterdam
29. Linder, M. (1991) *Nutritional Biochemistry and Metabolism*, p. 98, Elsevier Scientific Publishing Co., Inc., New York
30. Heinecke, J. W., Li, W., Daehnke, H. L., III, and Goldstein, J. A. (1993) *J. Biol. Chem.* **268,** 4069–4077
31. Giulivi, C., and Davies, K. J. A. (1993) *J. Biol. Chem.* **268,** 8752–8759
32. Huggins, T. G., Wells-Knecht, M. C., Detorie, N. A., Baynes, J. W., and Thorpe, S. R. (1993) *J. Biol. Chem.* **268,** 12341–12347
33. Davis, J. C., and Averill, B. A. (1981) *J. Biol. Chem.* **256,** 5992–5996
34. Davis, J. C., and Averill, B. A. (1984) *Inorg. Chim. Acta* **93,** L49-L51
35. Ikeda-Saito, M (1985) *J. Biol. Chem.* **260,** 11688–11696
36. Marquez, L. A., Huang, J. T., and Dunford, H. B. (1994) *Biochemistry* **33,** 1447–1454
37. Agner, K. (1958) *Acta Chem. Scand.* **12,** 89–94
38. Cotton, M. L., and Dunford, H. B. (1973) *Can. J. Chem.* **51,** 582–587
39. Nelson, D. P., and Kiesow, L. A. (1972) *Anal. Biochem.* **49,** 474–478
40. Malanik, V., and Ledvina, M. (1979) *Prep. Biochem.* **9,** 273–280
41. Ushijima, Y., Nakano, M., and Goto, T. (1984) *Biochem. Biophys. Res. Commun.* **125,** 916–918
42. Amado, R., Aeschbach, R., and Neukom, H. (1984) *Methods Enzymol.* **107,** 377–388
43. Bayse, G. S., Michaels, A. W., and Morrison, M. (1972) *Biochim. Biophys. Acta* **284,** 34–42
44. Segel, I. H. (1975) *Enzyme Kinetics: Behavior and Analysis of Rapid Equilibria and Steady State Enzyme Systems*, pp. 100–160, John Wiley and Sons, Inc., New York
45. Jensen, M. S., and Bainton, D. F. (1973) *J. Cell Biol.* **56,** 379–388
46. Harrison, J. E., Araiso, T., Palcic, M. M., and Dunford, H. B. (1980) *Biochem. Biophys. Res. Commun.* **94,** 34–40
47. Oertling, W. A., Hoogland, H., Babcock, G. T., and Wever, R. (1988) *Biochemistry* **27,** 5395–5400
48. Nomura, K., Suzuki, N., and Matsumoto, S. (1990) *Biochemistry* **29,** 4525–4534
49. Hunter, E. P. L., Desroisiers, M. F., and Simic, M. (1989) *Free Rad. Biol. & Med.* **6,** 581–585
50. Galeazzi, L., Groppa, G., and Giunta, S. (1990) *J. Clin. Microbiol.* **28,** 2145–2147
51. Butterworth, P. J. (1972) *Biochim. Biophys. Acta* **289,** 251–253
52. Ohtaki, S., Nakagawa, H., Nakamura, M., and Yamazaki, I. (1982) *J. Biol. Chem.* **257,** 761–766
53. Ralston, I., and Dunford, H. B. (1978) *Can. J. Biochem.* **56,** 1115–1119
54. Ralston, I. M., and Dunford, H. B. (1980) *Can. J. Biochem.* **58,** 1270–1276
55. Ohtaki, S., Nakagawa, H., Nakamura, M., and Yamazaki, I. (1982) *J. Biol. Chem.* **257,** 13398–13403
56. Joschek, H. I., and Miller, S. I. (1966) *J. Am. Chem. Soc.* **88,** 3273–3281
57. Lee, H. C., Booth, K. S., Caughey, W. S., and Ikeda-Saito, M. (1991) *Biochim. Biophys. Acta* **1076,** 317–320
58. Sealy, R. C., Harman, L., West, P. R., and Mason, R. P. (1985) *J. Am. Chem. Soc.* **107,** 3401–3406
59. Hori, H., Fenna, R. E., Kimura, S., and Ikeda-Saito, M. (1994) *J. Biol. Chem.* **269,** 8388–8392
60. Marquez, L. A., and Dunford, H. B. (1994) *J. Biol. Chem.* **269,** 7950–7956
61. Cornish-Bowden, A. (1974) *Biochem J.* **137,** 143–144
62. Bakkenist, A. R. J., De Boer, J. E. G., and Wever, R. (1980) *Biochim. Biophys. Acta* **613,** 337–348
63. Andrews, P. C., and Krinsky, N. I. (1982) *J. Biol. Chem.* **257,** 13240–13245
64. Bolscher, B. G. J. M., and Wever, R. (1984) *Biochim. Biophys. Acta* **788,** 1–10
65. Sibbett, S. S., and Hurst, J. K. (1984) *Biochemistry* **23,** 3007–3013

Kinetics of Oxidation of Tyrosine and Dityrosine by Myeloperoxidase Compounds I and II: IMPLICATIONS FOR LIPOPROTEIN PEROXIDATION STUDIES

Leah A. Marquez and H. Brian Dunford

J. Biol. Chem. 1995, 270:30434-30440.
doi: 10.1074/jbc.270.51.30434